Condensed Matter Physics, 1999, Vol. 2, No 2(18), pp. 319–328

CONDENSED MATTER PHYSICS

Fermi liquid properties of ^{3}He –^{4}He mixtures

K.Schörkhuber [1], E.Krotscheck [1], J.Paaso [2], M.Saarela [2], R.Zillich [1]

[1] Institut für Theoretische Physik, Johannes Kepler Universität A 4040 Linz, Austria

[2] Department of Physical Sciences, Theoretical Physics, University of Oulu, FIN-90570 Oulu, Finland

Received June 29, 1998

We calculate microscopically the properties of ^{3}He impurity atoms in ^{3}He-^{4}He mixtures, including the spectrum of a single particle and the Fermi–Liquid interaction between ^{3}He atoms. From these, we determine the pressure and concentration dependence of the effective mass and the magnetic susceptibility. The long wavelength limit of the single–particle spectrum defines the hydrodynamic effective mass. When $k \geqslant 1.7$Å^{-1} the motion of the impurity is damped due to the decay into a roton and a low energy impurity mode. The calculations of the Fermi–Liquid interaction are based on correlated basis functions (CBF) perturbation theory; the relevant matrix elements are determined by the Fermi hypernetted–chain summation method. Our theoretical effective masses agree well with recent measurements [1,2] but our analysis suggests a new extrapolation to the zero-concentration limit. With that effective mass we also find a good agreement with the measured [3] Landau parameter F_0^a.

Key words: *^{3}He-^{4}He mixtures, microscopic theory, Fermi–liquid interaction*

PACS: *67.40.Db, 67.60.-g, 67.70.Hr*

1. Introduction

Ground state properties like the energetics, local structure, and stability of the pure ^{3}He and ^{4}He, as well as the ^{3}He-^{4}He mixtures are well understood from the microscopic point of view [4]. Microscopic many-body theory postulates an empirical Hamiltonian that contains only a phenomenological two-body interaction [5] and the

masses of the particles,

$$H = -\sum_{\alpha}\sum_{i=1}^{N_\alpha}\frac{\hbar^2}{2m_\alpha}\nabla_{i,\alpha}^2 + \frac{1}{2}\sum_{\alpha\beta}{\sum_{i,j}}^{N_\alpha,N_\beta}{}' V(|\mathbf{r}_i^{(\alpha)} - \mathbf{r}_j^{(\beta)}|)\,. \tag{1}$$

One uses the Feenberg *ansatz* [6,7] for the ground state wave function,

$$\begin{aligned}\Psi_0(\{\mathbf{r}_i^{(\alpha)}\}) &= e^{\frac{1}{2}U(\{\mathbf{r}_i^{(\alpha)}\})}\Phi_0(\{\mathbf{r}_i^{(3)}\})\;; \\ U(\{\mathbf{r}_i^{(\alpha)}\}) &= \frac{1}{2!}\sum_{\alpha,\beta}{\sum_{i,j}}^{N_\alpha,N_\beta}{}' u^{\alpha\beta}(\mathbf{r}_i,\mathbf{r}_j) + \frac{1}{3!}\sum_{\alpha,\beta,\gamma}{\sum_{i,j,k}}^{N_\alpha,N_\beta,N_\gamma}{}' u^{\alpha\beta\gamma}(\mathbf{r}_i,\mathbf{r}_j,\mathbf{r}_k)\,.\end{aligned} \tag{2}$$

$\Phi_0(\{\mathbf{r}_i^{(3)}\})$ is a Slater determinant of plane waves ensuring the antisymmetry of the Fermion component of the mixture. The superscripts α, β, ... refer to the type of particles; the prime on the summation symbol in equations (1), (2) indicates that no two pairs (i,α), (j,β) can be the same. The correlation functions $u^{\alpha\beta}(\mathbf{r}_i,\mathbf{r}_j)$ and $u^{\alpha\beta\gamma}(\mathbf{r}_i,\mathbf{r}_j,\mathbf{r}_k)$ are determined by the functional minimization of the ground state energy [7,4]. The theory reproduces the experimental equation of state of ^{3}He-^{4}He mixtures [8] typically within 0.01 K.

2. Single impurity spectrum

The properties of single ^{3}He atoms moving in liquid ^{4}He are dominated by hydrodynamic backflow [9,10] of the ^{4}He liquid. To deal with a moving ^{3}He impurity, one must allow for *time-dependent* correlations between a single impurity and the ^{4}He host liquid; in other words the variational wave function of a moving ^{3}He impurity with coordinate $\mathbf{r}_0$ is

$$\begin{aligned}\Phi(\mathbf{r}_0,\mathbf{r}_1,...\mathbf{r}_N;t) &= \mathrm{e}^{-\mathrm{i}E_{N+1}t/\hbar}\,\frac{\Psi^{(3)}(\mathbf{r}_0,\mathbf{r}_1,...\mathbf{r}_N;t)}{\sqrt{\langle\Psi^{(3)}(t)\mid\Psi^{(3)}(t)\rangle}}\,, \\ \Psi^{(3)}(\mathbf{r}_0,\mathbf{r}_1,...\mathbf{r}_N;t) &= \mathrm{e}^{\frac{1}{2}\left[\delta u^{(3)}(\mathbf{r}_0;t)+\sum_{i=1}^{N}\delta u^{(34)}(\mathbf{r}_0,\mathbf{r}_i;t)\right]}\Psi_0^{(3)}(\mathbf{r}_0,\mathbf{r}_1,...,\mathbf{r}_N)\;.\end{aligned} \tag{3}$$

Here, E_{N+1} is the variational ground state energy of the $N+1$ particle system. The time–dependent components of the wave function are determined by an action principle, searching for a stationary value of the action integral

$$\delta\mathcal{S} = \delta\int \mathrm{d}t\;\langle\Phi(t)|H^{(3)} + U_{\mathrm{ext}}(\mathbf{r}_0;t) - \mathrm{i}\hbar\frac{\partial}{\partial t}|\Phi(t)\rangle = 0\;, \tag{4}$$

where $H^{(3)}$ is the Hamiltonian of the impurity-background system, obtained from equation (1) for $N_3 = 1$, and $U_{\mathrm{ext}}(\mathbf{r}_0;t)$ a weak external potential driving the impurity motion. Linearization of the resulting equations of motion leads to an implicit equation for the excitation spectrum of the form

$$\hbar\omega = t_3(k) + \Sigma(k,\omega)\,. \tag{5}$$

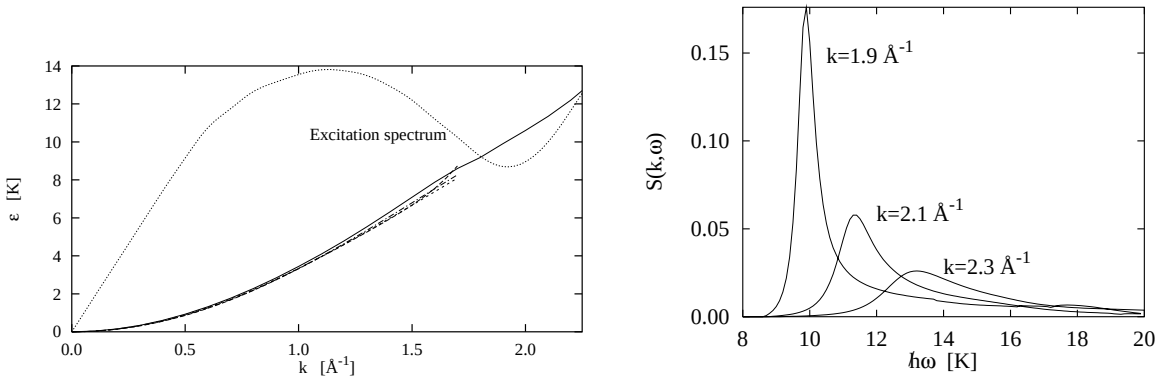

Figure 1. The left figure shows the excitation spectrum of a ^{3}He impurity. The solid curve is our theoretical result. It is compared with the data of [11–13] and the phonon–roton spectrum [14] (dotted line). The right figure shows the dynamic structure function at indicated momentum transfers where the spectrum is broadened.

Here $t_3(k) = \hbar^2 k^2/2m_3$ and the self–energy $\Sigma(k,\omega)$ describes the interaction with the background, which is due to hydrodynamic backflow. [10,15] For $0 \leqslant k \leqslant 1.7$ Å^{-1} the spectrum is sharp and defines a weakly momentum–dependent *hydrodynamic effective mass* $m_{\rm H}(k)$. Theory and experiments in this regime agree quite satisfactorily, *cf.* figure 1. At shorter wavelengths, the impurity couples to the roton and thus the spectrum broadens.

3. Microscopic Fermi liquid theory

The interaction between pairs of ^{3}He impurities causes a concentration dependence of the effective mass [1,2] and the magnetic susceptibility [3]. When the ^{3}He atoms are close to the Fermi surface, these interactions are described by Landau's Fermi liquid theory. The single particle spectrum and the quasiparticle interaction at the Fermi surface are obtained from the variations

$$\epsilon^{(3)}(k) = \delta E_0/\delta n_k \tag{6}$$

and

$$N(0)\ \left.\frac{\delta^2 E_0}{\delta n_{\mathbf{k},\sigma}\delta n_{\mathbf{k}',\sigma'}}\right|_{n_k^{(0)}} = F_{\sigma,\sigma'}(\mathbf{k},\mathbf{k}') = \sum_\ell \left[F_\ell^{\rm s} + \sigma\cdot\sigma' F_\ell^{\rm a}\right] P_\ell(\hat{\mathbf{k}}\cdot\hat{\mathbf{k}}') \tag{7}$$

evaluated for the ground state $n_k^{(0)}$. $N(0) = \Omega\, m^*\, k_{\rm F}/\pi^2\,\hbar^2$ is the density of states at the Fermi surface. Equation (7) defines Landau's Fermi–liquid parameters $F_\ell^{\rm (s,a)}$.

Within the framework of the wave function (2), quasiparticle properties are calculated by variation with respect to the occupation n_k of orbitals in the Slater determinant Φ_0. The techniques of the (Fermi)-hypernetted chain ((F)HNC) theory

[4] are used for calculating the relevant diagrams. For the dilute ^{3}He component, the spectrum has the simple Hartree–Fock form

$$\epsilon^{(3)}(k) = t_3(k) + u(k) + U_0, \quad u(k) = -\int \frac{\mathrm{d}^3 q}{(2\pi)^3 \rho^{(3)}}\, n_{|\mathbf{q}-\mathbf{k}|,\sigma}\, \tilde{W}_{\mathrm{eff}}(q)\,, \tag{8}$$

where $\tilde{W}_{\mathrm{eff}}(q)$ is a local effective potential giving rise to the average field $u(k)$, and U_0 is a constant. The quasiparticle interaction is the antisymmetrized matrix element of the same effective potential $W_{\mathrm{eff}}(q)$.

Fermi liquid parameters derived from the wave function (2) do not agree well with experiments. The cure for the problem is correlated-basis functions (CBF) theory [6] to infinite order [16]. The method uses the correlations $u_n(\mathbf{r}_1, \ldots, \mathbf{r}_n)$ to generate a basis of the Hilbert space which is then used for perturbation theory; it can be mapped on a Green's function approach in terms of effective interactions that are provided by the variational theory.

In CBF theory, the single particle properties are again described by a complex self-energy $\Sigma(k, E)$; and the single particle spectrum is obtained from an equation of type (5). If only one-phonon coupling processes are considered, $\Sigma(k, E)$ is given by the so-called G0W-approximation [17]

$$\Sigma(k, E) = \mathrm{i} \int \frac{\mathrm{d}^3 q \mathrm{d}(\hbar\omega)}{(2\pi)^4 \rho^{(3)}} G^{(0)}(|\mathbf{k}-\mathbf{q}|\,, \frac{E}{\hbar} - \omega) \tilde{V}_{\mathrm{eff}}(q, \omega). \tag{9}$$

$$\begin{aligned} G^{(0)}(k,\omega) &\equiv G^{(0)}_{\mathrm{H}}(k,\omega) + G^{(0)}_{\mathrm{F}}(k,\omega) \\ &= \frac{1}{\hbar\omega - t_3(k) + \mathrm{i}\eta} + n^{(0)}_k \left[\frac{1}{t_3(k) - \hbar\omega - \mathrm{i}\eta} - \frac{1}{t_3(k) - \hbar\omega + \mathrm{i}\eta} \right] \end{aligned} \tag{10}$$

is the free single-particle Green's function and

$$\tilde{V}_{\mathrm{eff}}(q,\omega) = \tilde{V}^{33}_{\mathrm{p-h}}(q) + \sum_{\alpha\beta} \tilde{V}^{3\alpha}_{\mathrm{p-h}}(q) \chi_{\alpha\beta}(q,\omega) \tilde{V}^{3\beta}_{\mathrm{p-h}}(q)\,. \tag{11}$$

The particle-hole irreducible interactions $\tilde{V}^{\alpha\beta}_{\mathrm{p-h}}(q)$ are provided by the variational ground state theory; $\chi_{\alpha\beta}(q,\omega)$ is the density-density response matrix.

The Green's function has been written in the form (10) to separate the "hydrodynamic" and the "fermionic" part. Correspondingly, we write the the self-energy as $\Sigma(k, E) = \Sigma_{\mathrm{H}}(k, E) + \Sigma_{\mathrm{F}}(k, E)$. The "hydrodynamic" part $\Sigma_{\mathrm{H}}(k, E)$ of the self-energy is an approximation to the one used in section 2, and

$$\Sigma_{\mathrm{F}}(k, E) = -\int \frac{\mathrm{d}^3 q}{(2\pi)^3 \rho_3} n^{(0)}_q \tilde{V}_{\mathrm{eff}}(\mathbf{k}-\mathbf{q}, (E - t_3(q))/\hbar)\ . \tag{12}$$

The difference to the static theory is the *energy dependence* of $\tilde{V}_{\mathrm{eff}}(q,\omega)$. Indeed, the expression (8) can be derived from equation (12) using the same "average-energy"

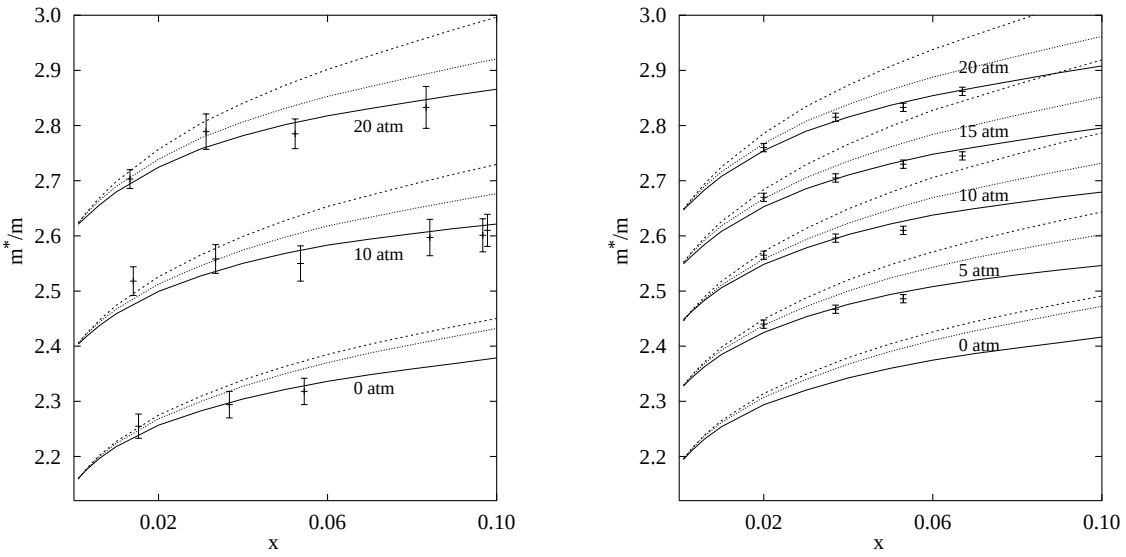

Figure 2. Theoretical and experimental effective mass ratio $m^*(P,x)/m$ as a function of the concentration. The full curve is the fully self-consistent result, the dotted curve is the result without retardation effects, the short dashed curve represents the static approximation. Symbols with error bars refer to the data of [2] in the left figure and [1] in the right figure.

procedure that has been employed to establish the connection between the parquet-diagram theory and the optimized HNC theory [18]. However, the quasiparticle interaction *should* be calculated for $\omega = 0$.

Three calculations have been carried out to determine the Fermi liquid contributions to the effective mass of the ^{3}He component as a function of concentration and pressure. The first calculation applied the simple FHNC/EL theory and the static effective interaction (8). To account for the hydrodynamic backflow, one must supplement the Fermion contribution (6) by the hydrodynamic contribution $\hbar\omega_{\mathrm{H}}(k)$; then the spectrum has the form

$$\epsilon^{(3)}(k) = \hbar\omega_{\mathrm{H}}(k) + u(k) + U_0 \ , \tag{13}$$

where the Fermi correction $u(k)$ is given in equation (8). When treated this way, the concentration dependence of the effective mass derived from the spectrum (13) is visibly steeper than the experimental one, as seen in figure 2.

In the next step, we calculate the effective mass using $\tilde{V}_{\mathrm{eff}}(\mathbf{k},0)$ as quasiparticle–interaction. This form of the self-energy relaxes the approximations made by the FHNC theory since it takes the effective interaction at the Fermi surface and not at an average energy. We see in figure 2 that the agreement with the experiment is indeed improved; the approximation recovers about half of the discrepancy between the FHNC approximation and the experiments.

Finally, we have carried out self-consistent calculations of the effective mass. It is sufficient for that purpose to assume a single-particle spectrum of the form $t^{(3)}(k) = \hbar^2k^2/2m^*$ in the Green's function (10) and, consequently, in equation (12);

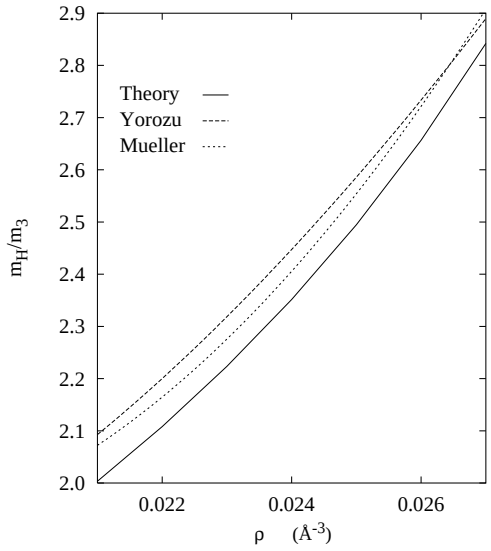

Figure 3. The figure shows the theoretical (thick full and dashed curves) and experimental (circles [1] and boxes [2] with error bars) effective mass ratio $m^*(P,x)/m$ as a function of pressure P (in atm) and concentration x. Also shown is the static approximation (short dashed curves.)

note that the hydrodynamic mass is included in the Green's function. This effective mass is then determined self-consistently by requiring that the spectrum $\epsilon^{(3)}(k)$ determined by

$$\epsilon^{(3)}(k) = \hbar\omega_{\rm H}(k) + \Sigma_{\rm F}\left(k, \frac{\hbar k^2}{2m^*}\right) \tag{14}$$

can be fitted by the same effective mass that has been used in the self-energy. This calculation provides a very good agreement with the experimental data as seen in figure 2. The agreement is worst for the pressure 10 atm and the data of [2]; but we note that there is a non-monotonic behaviour of the slope of the data as a function of pressure, and it might be interesting to re-examine this pressure regime experimentally.

Although the results of section 2 for the hydrodynamic effective mass are quite satisfactory we have allowed the hydrodynamic mass to be a free parameter in the further calculations in order to eliminate any uncertainty. We have calculated the concentration dependence of the effective mass from the Fermi-liquid contributions and then made a single parameter fit to the experiments of [1] and [2] to optimize the overall agreement. Extrapolating this fit to zero concentration, we arrived at the interpolation formulas

$$\frac{m_{\rm H}}{m_3}\Bigg) = 2.18 + 2.43\,r + 2.67\,r^2 - 1.17\,r^3 \tag{15}$$

or

$$\frac{m_{\rm H}}{m_3}\Bigg) = 2.15 + 2.16\,r + 4.47\,r^2 \tag{16}$$

Table 1. Pressure dependence of the coefficients of the expansion (17) for the concentration dependence of the effective mass. The expansion coefficients a, b, c, and d are from [19].

P (atm)	a	b	c	d
0	1.49	1.39	–18.2	36.7
5	1.07	3.00	–22.6	40.2
10	0.789	4.48	–28.2	50.4
15	0.501	6.17	–36.1	66.8
20	0.310	7.41	–42.1	80.1

for the hydrodynamic mass of [1] and [2], respectively. Here, $r = \rho_4/\rho_0 - 1$, ρ_4 is the ^{4}He density and $\rho_0 = 0.02183\,\text{Å}^{-3}$ is its value at saturation.

The results for the hydrodynamic mass from both extrapolations as well as our theoretical calculations of section 2 are shown in figure 3. Typically, the discrepancy between the two different extrapolations is 0.03, the theoretical values are 0.05-0.1 below those.

Since the calculations were done for fixed densities at each concentration and the experiments were done for a fixed pressure, we have used the experimental pressure-density relation of [8] to make the conversion. Our calculations predict, at low concentration, a visible curvature of the effective mass as a function of concentration. Hence, we are not convinced that linear extrapolations are a legitimate means to determine the hydrodynamic mass unless concentrations are used that are significantly lower than those examined in [2]. Such a curvature is implicit to the Fermi functions. Already the simple approximation (13) would lead to a behaviour

$$m^*(x) = m^*_{\text{H}} + ax^{2/3} + bx + cx^{5/2} + dx^{7/3} \ldots \,. \tag{17}$$

The numerical coefficients $a \ \ldots \ d$ can be calculated from the moments of the potential, but such an expansion provides valid results only for very small concentrations and thus a global fit of the form (17) to the calculated data is more accurate. In table 1 we list their values for different pressures obtained from the least square fit to the fully self-consistent solution of equation (14).

Table 2. Pressure dependence of the parameters of the fit (19) of the unnormalized Fermi liquid parameter $(m/m^*)F_0^{\text{a}}$ as obtained from the dynamic calculation.

P (atm)	a	b	c	d
0	0.447	–4.371	14.67	–22.35
5	0.394	–3.710	10.82	–14.73
10	0.362	–3.319	8.410	–9.660
15	0.344	–3.012	6.336	–4.927
20	0.326	–2.733	4.383	–0.349

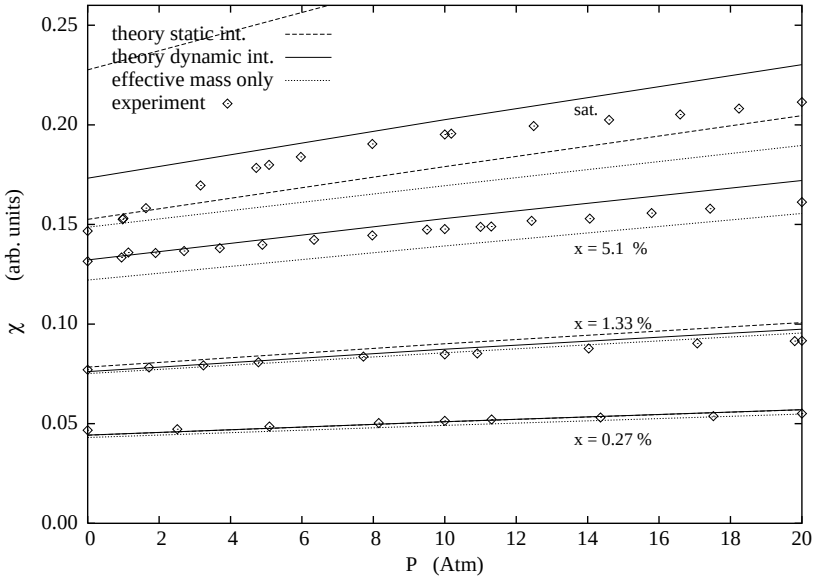

Figure 4. The figure shows a comparison between experimental (diamonds, from figure 1 of [3]) and theoretical magnetic susceptibilities. The theoretical results were scaled to generate the best overall fit to the data at 0.27 % and 1.33 % concentration. The solid lines are the results of the full microscopic calculation and the long dashed lines are the results from using the static interaction $\tilde{W}_{\rm eff}(q)$. The static results for 8.8 % concentration are off-scale.

The same effective interaction and the corresponding effective masses were used to compute the magnetic susceptibility

$$\frac{\chi^*_{\rm ideal}}{\chi} = \frac{m_{\rm H}}{m^*}\ (1 + F_0^{\rm a})\ . \tag{18}$$

We show in figure 4 a comparison between theoretical and experimental results. Again, it is seen that the dynamic CBF theory reproduced the experiments quite well, whereas the static FHNC result is generally worse than the "non-interacting" result where the Landau parameter $F_0^{\rm a}$ is simply omitted. Similar to the fit (17) for the effective mass, one can make a concentration expansion for the antisymmetric Landau parameter. Since the definition of the Landau parameters suggest a natural factorization into an effective mass ratio and an interaction term, we expand

$$\frac{m}{m^*}\ F_0^{\rm a}(x) = a\ x^{1/3} + b\ x + c\ x^{5/3} + d\ x^{7/3}\ . \tag{19}$$

The density–dependent parameters entering this fit are given in table 2.

In concluding we find satisfactory agreement with the measured effective mass and magnetic susceptibility of the ^{3}He component of a ^{3}He-^{4}He mixture within a unified theoretical picture. We have also demonstrated that the naïve application of variational wave functions leads to unsatisfactory results and have shown that this shortcoming is due to the effective interaction taken at the incorrect energy.

Furthermore, retardation effects have a notable influence on the effective mass of the fermion component.

Acknowledgements

The work was supported, in part, by the Austrian Science Fund under project P11098-PHY, and the Academy of Finland.

References

1. Yorozu S., Fukuyama H., Ishimoto H. Isochoric pressure and ^{3}He quasiparticle effective mass in a ^{3}He-^{4}He mixture under pressure. // Phys. Rev B, 1993, vol. 48, p. 9660.
2. Simons R., Mueller R.M. Specific heat of ^{3}He-^{4}He-mixtures at low temperatures and high ^{3}He concentration. // Czekoslowak Journal of Physics Suppl., 1996, vol. 46, p. 201.
3. Ahonen A.I., Paalanen M.A., Richardson R.C., Takano Y. The magnetic susceptibility of dilute mixtures of ^{3}He in liquid ^{4}He. // J. Low Temp. Phys., 1976, vol. 25, p. 733.
4. Krotscheck E., Saarela M. Theory of ^{3}He-^{4}He mixtures: energetics, structure, and stability. // Phys. Rep., 1993, vol. 232, p. 1.
5. Aziz R.A. *et. al.* An accurate intermolecular potential for helium. // J. Chem. Phys., 1979, vol. 70, p. 4330.
6. Feenberg E. Theory of Quantum Fluids. New York, Academic, 1969.
7. Campbell C.E. Progress in Liquid Physics. London, Wiley, 1977.
8. de Bruyn Ouboter R., Yang C.N. The thermodynamic properties of liquid ^{3}He-^{4}He mixtures between 0 and 20 atm in the limit of absolute zero temperature. // Physica, 1986, vol. 144B, p. 127.
9. Landau L.D., Pomeranchuk I. On the Motion of Foreign Particles in Helium II. In: Collected Papers of L. D. Landau. New York, Gordon and Breach, 1967.
10. Feynman R.P., Cohen M. Energy spectrum of the excitations in liquid helium. // Phys. Rev., 1956, vol. 102, p. 1189.
11. Greywall D.S. Experimental determination of the ^{3}He-quasiparticle excitation spectrum for dilute solutions of ^{3}He in superfluid ^{4}He. // Phys. Rev. B, 1979, vol 20, p. 2643.
12. Fåk B. *et al.* Elementary excitations in superfluid ^{3}He-^{4}He mixtures: Pressure and temperature dependence. // Phys. Rev. B, 1990, vol. 41, p. 8732.
13. Owers-Bradley J.R., Main P.C., Bowley R.M., Batey G.J., Church R.J. // J. Low Temp. Phys., 1988, vol. 72, p. 201.
14. Cowley R.A., Woods A.D.B. Inelastic scattering of thermal neutrons from liquid helium. // Can. J. Phys., 1971, vol. 49, p. 177.
15. Owen J.C. Microscopic calculation of the low-temperature properties of ^{3}He-^{4}He mixtures. // Phys. Rev. B, 1981, vol. 23, p. 5815.
16. Krotscheck E. Effective interactions, linear response, and correlated rings: A study of chain diagrams in correlated basis functions. // Phys. Rev. A, 1982, vol. 26, p. 3536.
17. Hedin L. New method for calculating the one-particle Green's function with application to the electron-gas problem. // Phys. Rev. A, 1965, vol. 139, p. 796.

18. Jackson A.D., Lande A., Smith R.A. Plenar theory made variational. // Phys. Rev. Lett., 1985, vol. 54, p. 1469.
19. Krotscheck E., Saarela M., Schörkhuber K., Zillich R. Concentration dependence of the effective mass of ^{3}He atoms in ^{3}He-^{4}He mixtures. // Phys. Rev. Lett, 1997, vol. 80, p. 4709.

Фермі рідинні властивості сумішей ^{3}He – ^{4}He

К.Шойркхубер [1], Е.Крочек [1], Дж.Паасо [2], М.Саарела [2], Р.Ціллі [1]

[1] Інститут теоретичної фізики, університет Йогана Кеплера 4040 Лінц, Австрія

[2] Факультет фізичних наук, відділ теоретичної фізики університет Оулу, FIN-90570 Оулу, Фінляндія

Отримано 29 червня 1998 р.

Проведено мікроскопічне дослідження властивостей домішкових атомів ^{3}He у сумішах ^{3}He-^{4}He, зокрема, розраховано одночастинковий спектр та Фермі рідинну взаємодію для атомів ^{3}He. На цій основі знайдені залежності ефективної маси і магнітної сприйнятливості від тиску і концентрації. Гідродинамічна ефективна маса визначається з довгохвильової границі одночастинкового спектру. Для $k \geqslant 1.7$ Å^{-1} рух домішки в силу розпаду на ротон та низькоенергетичне домішкове збудження є утруднений. Розрахунки Фермі рідинної взаємодії базувалися на теорії збурень з корельованими базисними функціями; відповідні матричні елементи розраховувалися методом ферміонного гіперланцюжкового сумування. Теоретично отримані ефективні маси добре узгоджуються з недавніми вимірюваннями [1,2], водночас проведений аналіз дозволив запропонувати нову екстраполяційну формулу для границі нульової концентрації. При цьому знайдено також добре узгодження з параметром Ландау F_0^a, виміряним в [3].

Ключові слова: *суміші ^{3}He-^{4}He, мікроскопічна теорія, взаємодія в фермі-рідині*

PACS: *67.40.Db, 67.60.-g, 67.70.Hr*